

Field Map Based Automated Shimming For Organs Outside of the Human Brain

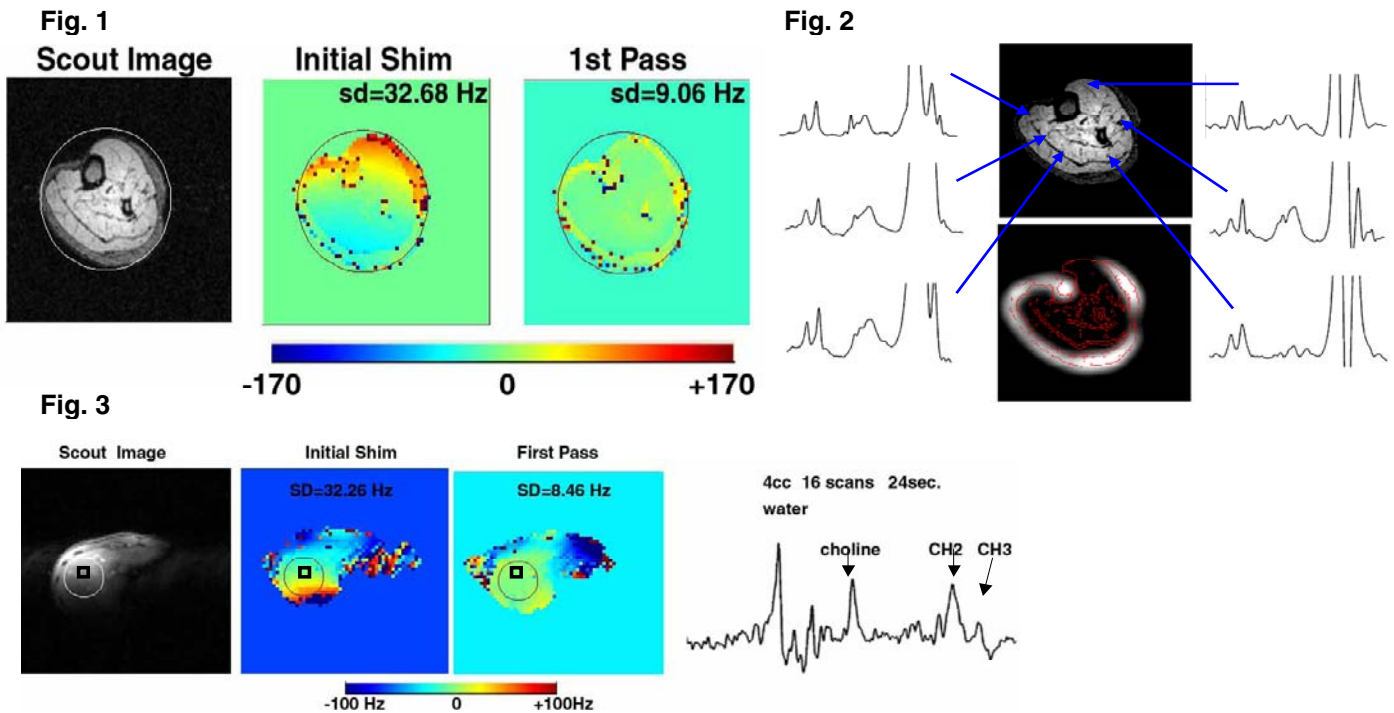
H. P. Hetherington¹, N. I. Avdievich¹, J. W. Pan²

¹Radiology, Albert Einstein College of Medicine, Bronx, NY, United States, ²Neurology, Albert Einstein College of Medicine, Bronx, NY, United States

Introduction: For the brain, a variety of automated non-iterative shimming methods using phase evolution derived B_0 maps have been reported. These methods assume that there is only a single chemical species contributing to the image. Although this is true in the brain, lipid contributions from skin, bone marrow and structural fat, may approach or exceed the local concentration of water in the leg and liver. In these instances, standard B_0 mapping methods cannot be used due to the phase/frequency contribution arising from the lipids. To overcome these limitations we have developed a multi-point B_0 mapping combined with Dixon imaging to provide fully automated shimming of the human calf and liver.

Methods: B_0 maps were obtained using a multi-slice (11 slices, 2mm thick/2mm gap) gradient echo imaging sequence (64x64 resolution, FOV 192x192mm) with 6 B_0 evolution delays (0,0.9,1.8,2.7,4.5 and 8.1ms). All 6 B_0 evolution times were acquired with each phase encoding step (66 slices per TR, 1500ms) resulting in a total measurement time of 96seconds. The first three B_0 delays are used to calculate a three point Dixon image. From this data the intensity, A_{msd} , in any pixel is given by $A_{msd}\exp(-i\phi_{msd}) = A_w\exp(-i\phi_w) + A_f\exp(-i(\phi_{wf} + \phi_w))$ where A_w and A_f are the amplitudes of the water and fat signals, ϕ_w is the phase due to the B_0 field and ϕ_{wf} is the phase due to the chemical shift difference between fat and water. Using A_w and A_f , as determined from the three point Dixon images, ϕ_w can be determined and the B_0 map calculated. The B_0 map is then fit as a sum of spherical harmonics (1st - 3rd order). These values are then scaled and uploaded to the shim amplifiers.

Results: Displayed in Fig. 1 are a scout image showing the target ROI (white circle) and the B_0 maps prior to shimming and after a single iteration. The frequency values are color-coded according to the scale. There is a dramatic reduction in the SD of the water frequency decreasing from 32.68 Hz to 9.06Hz in a single pass. Displayed in Fig. 2 are spectroscopic imaging data after shimming, including water and fat images. There is excellent resolution between the choline and creatine resonance throughout the entire leg. Fig. 3 displays the scout image of the liver (acquired with a surface coil) along with the target ROI for shimming (white circle) and the selected volume (black square). Also displayed in Fig. 3 are the B_0 maps acquired before and after shimming, showing a dramatic reduction in SD from 32.26 to 8.46Hz using a single iteration. Also displayed is a liver spectrum, 4cc (black square), using 16 scans without respiratory gating.



Conclusions: The method described enables fully automated shimming even in locations where the lipids exceed the water such as in the leg and liver in a single pass.